

THERMODYNAMIC AND KINETIC SIMULATION OF Y_2O_3 AND Y_2S_3 NONMETALLIC PHASE FORMATION IN LIQUID STEEL

S. Gerasin, D. Kalisz*, J. Iwanciw

* AGH University of Science and Technology, Faculty of Foundry Engineering, Kraków, Poland

(Received 26 March 2019; accepted 30 August 2019)

Abstract

The current work deals with the phenomenon of non-metallic inclusions as a result of the addition of yttrium to the liquid steel as an alloying component. The order of introducing individual components determines their final content in steel, and this problem was analyzed using the WYK_Stal program developed at AGH. The study of Y_2O_3 and Y_2S_3 phase precipitation and the relationship between the addition of Y, Al, Ca, O, and S in molten steel was studied using the thermodynamic models based on Wagner's formalism. The introductions of yttrium prior to aluminum brought about huge losses, and it mainly occurred due to the formation of oxides. The low oxygen content in the metal bath promotes the formation of yttrium sulphide. When yttrium is introduced after aluminum and calcium, yttrium is used for the precipitation of its sulfide, and in this way the manganese sulfide formation is reduced.

Keywords: Yttrium; Non-metallic precipitate; Steel; Computer simulation

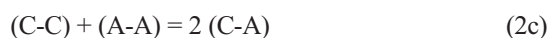
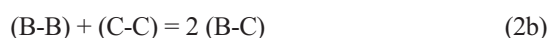
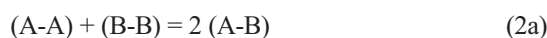
1. Introduction

The non-metallic phase being formed in liquid steel during its deoxidization mainly consists of iron oxides, manganese oxides, silica oxides, and aluminum oxides, and it is considered to be an oxide phase [1-4]. Its thermodynamic properties can be described twofold: by an expression for the activity of components of liquid solutions or as an expression for free energy of mixing. What is common for these two description methods is the mathematical dependency of different complexity level, when more components are involved. These methods are derived from a definite ionic liquid model. The simplest model of regular solution [4] treats liquid oxide phase as a composition of two sub-networks: anionic, built only of O^{2-} ions, and cationic sub-network, which is treated as a regular solution. The value of regular solution parameter α_{ij} is defined for each two-component solution $i - j$, and the dependency for a multi-component solution assumes the below form [4]:

$$RT \cdot \ln \gamma_i = \sum_j \alpha_{ij} \cdot X_j^2 + \sum_j \sum_k (\alpha_{ij} + \alpha_{ik} - \alpha_{jk}) \cdot X_j \cdot X_k \quad (1)$$

Equation (1) shows a relation for the activity coefficient of a solution component. The activity is referred to the pure component. The solution is made of many oxides, the particle of which contains 1 metal atom.

A much more advanced solution is represented by the quasichemical model. The following example shows a model for a three-component system, e.g. AOx-BOy-CO₂, where it analyzes formation of pairs of atoms, i.e. associates in the cationic sub-network (closest neighbors) [5-7]:



Thus the cationic sub-network in the AOx-BOy solution consists of pairs of cations A, B and cationic associates AB.

The change of Gibbs' free energy for these elementary reactions calculated for 1 mole of component assumes the following form:

$$\Delta g_{AB} = \varpi_{AB} - \eta_{AB} \cdot T \quad (3a)$$

$$\Delta g_{BC} = \varpi_{BC} - \eta_{BC} \cdot T \quad (3b)$$

$$\Delta g_{CA} = \varpi_{CA} - \eta_{CA} \cdot T \quad (3c)$$

The equilibrium constant for the reaction of associate formation equals to [5-7]:

$$K_{ij} = \frac{X_{ij}^2}{X_{ii} \cdot X_{jj}} = 4 \cdot \exp \left[-\frac{2 \cdot (\varpi_{ij} - \eta_{ij} \cdot T)}{z \cdot R \cdot T} \right] \quad (4)$$

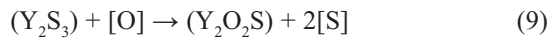
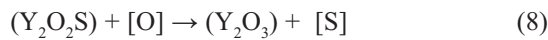
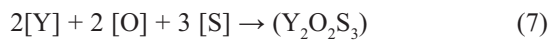
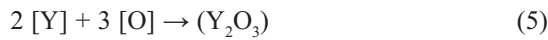
*Corresponding author: dak@agh.edu.pl



where z is the coordination number.

The formula for equilibrium constant and balance equation can be used for determining participation of particular structural units, and as a consequence, also free energy of mixing for a solution with metal ions and their associates. This model was used in the commercial program FactSage for calculating, e.g. interface equilibria.

The formation of non-metallic precipitates containing yttrium can be described with the following general equations [8-9]:



The compounds formed by yttrium and oxygen and sulphur can be identified in the form of YS, Y_2S_3 , Y_5S_7 , Y_3S_4 , Y_2S_4 , and Y_2O_2S . The generated non-metallic precipitates are small (0.5-3.0 μm) and evenly distributed in the ingot. Unlike big precipitates, Al_2O_3 or MnS (II and III type), they have high melting temperature: 1690-2291 $^\circ\text{C}$ for oxides, 1795-2450 $^\circ\text{C}$ for sulfides, and 1490-1990 $^\circ\text{C}$ for oxysulfides, which guarantees their durability [8-9]. The physicochemical properties of selected compounds based on yttrium are presented in Table 1.

Analogous to data presented in Table 1, the Fe-Y-S-O phase equilibrium system for temperature 1600 $^\circ\text{C}$ was given in Fig. 1. This plot creates bases for predicting order and type of phases formed as an effect of reaction of yttrium with oxygen and sulphur in liquid steel [10].

Based on this, the authors [10] determined stability conditions of particular phases:

$$\text{for } Y_2O_3: \quad a(S)/a(O) < 16; \quad a(O)^{3/2}a(Y) > 6.8 \cdot 10^{-8}$$

$$\text{for } Y_2O_2S: \quad 16 < a(S)/a(O) < 245; \quad a(O)^{3/2}a(Y) < 6.8 \cdot 10^{-8}$$

$$\text{for } Y_2S_3: \quad a(S)/a(O) > 245; \quad a(Y) < 10^{-3}, \quad a(S) > 0.06$$

$$\text{for } YS: \quad a(S)/a(O)^2 > 9.1 \cdot 10^{-5}; \quad a(Y) > 10^{-3}, \quad a(S) < 0.06$$

Precipitates are primarily formed as a result of reactions with oxygen, therefore the first compounds which should be precipitated are Y_2O_3 . They are formed simultaneously with oxysulfides Y_2O_2S [10]. The yttrium sulfide YS phase formation is associated with the highest activity of yttrium, and lower or very low activity of oxygen. However in the presence of other elements of high chemical affinity to oxygen or sulphur, e.g. Al, Ce, or Mn, the problem of yttrium dosing can be solved through numerical calculations. For obtaining reliable thermodynamic data on the stability of yttrium compounds and information about the interaction of complex phases, e.g. oxides in its presence, one should consider basic phase systems containing yttrium oxide. The analysis of data obtained by authors [10] reveals that after introducing yttrium and aluminum to steel at temperature 1600 $^\circ\text{C}$, the deoxidation products can also contain solid precipitates Y_2O_3 , $3Y_2O_3 \cdot 5Al_2O_3$, Al_2O_3 , and liquid oxidic phases. The addition of calcium and yttrium results in the formation of Y_2O_3 , $3CaO_2 \cdot Y_2O_3$, $CaO \cdot Y_2O_3$, $CaO \cdot Y_2O_3$, $CaO_2 \cdot Y_2O_3$, and liquid oxidic phases.

2. Computer program to simulation the refining process and introduce of alloying into liquid steel

The computer software for steel refining was based on its previous version (WYK_STAL), worked out by J. Iwanciw [11-15]. The reaction of deoxidizer dissolved in steel with dissolved oxygen can be written as a general equation:

Table 1. Standard Gibbs' energy and equilibrium constant of yttrium reaction for temperatures 1575–1625 $^\circ\text{C}$ [8]

Reaction	$J \cdot \text{mol}^{-1}$ $\Delta G^\circ = C - DT$		$\log K = -\left(\frac{A}{T}\right) + B$	
	$10^{-6} C$	$10^{-3} D$	$10^{-4} A$	B
$Y_2O_3(s) = 2[Y] + 3[O]$	1.793	0.658	9.365	34.4
$Y_2O_2S(s) = 2[Y] + 2[O] + [S]$	1.521	0.536	7.949	28.03
$Y_2S_3(s) = 2[Y] + 3[S]$	1.171	0.441	6.119	23.1
$YS(s) = [Y] + [S]$	0.321	0.091	1.677	4.74
$YN(s) = [Y] + [S]$	0.391	0.15	2.044	7.86
$YC_2(s) = [Y] + 2[C]$	1.704	0.124	0.809	6.49



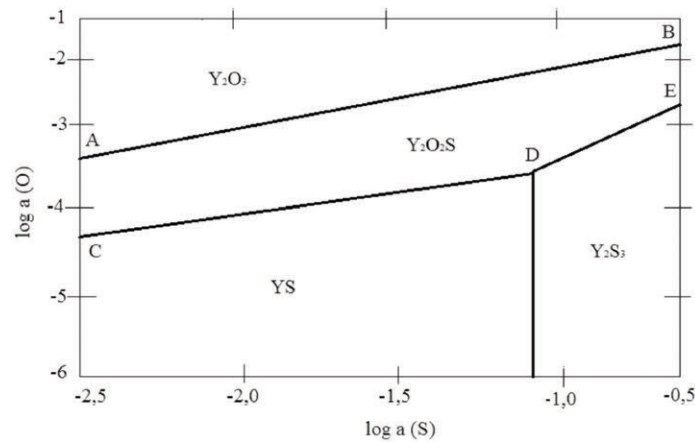


Figure 1. Phase equilibrium system of Fe-Y-S-O at temperature 1600°C [10]



The product of this type of process, i.e. $R_m O_n$, is dissolved in oxidic phase or appears as pure solid oxide, which may be part of a compound precipitate.

$$K_{(1)} = \frac{X_{R_m O_n} \cdot \gamma_{R_m O_n}}{([\%R] \cdot f_R)^m \cdot ([\%O] \cdot f_O)^n} \quad (11)$$

where: f_R and f_O are coefficients of activity (Henry's law) at concentrations [%R] and [%O] expressed in wt%; $X_{R_m O_n}$ stands for a molar fraction $R_m O_n$ treated as a chemical compound in liquid oxidic phase; and $\gamma_{R_m O_n}$ - coefficient of activity (Raoult's law). Constant of equilibrium (11) simultaneously makes use of activities of Raoult's and Henry's type [4, 16-17].

The program is used for calculating the present weight and chemical composition of reacting phases in any moment of the process. The simplest way of presenting changes of reagent concentrations in time is to describe the oxidic precipitate formation with kinetic equation of the first order.

$$\frac{dC}{dt} = -k \cdot (C - C_{eq}) \quad (12)$$

where: the C_{eq} concentration refers to the equilibrium of reaction, and k is the constant of velocity.

According to the generally assumed picture of steel deoxidation and its impact on the rate of the process, the hydrodynamic conditions resulting from the speed of mixing are of special significance. In the classical approach, the transport of the reagent to the place of reaction consists of two stages: convection, in which reagent is entrained by the whole volume of liquid metal, and diffusive in which reagent diffuses through the boundary layer of the concentration. The concentration of oxygen and deoxidant changes along the thickness of diffusion layer from the average value for liquid steel (in a given moment) to a value corresponding to the equilibrium of reaction of non-

metallic precipitate formation, in line with reaction (10).

Based on the above circumstances as in [11-13], the following form of kinetic equation of deoxidation was assumed [13]:

$$\frac{d[\%O]}{dt} = B_m \cdot D_R \cdot ([\%O] - [\%O]_{eq}) \quad (13)$$

where: [%O]- average concentration of oxygen in liquid steel (wt%)

$[\%O]_{eq}$ - oxygen concentration after reactions corresponding to equilibrium of reaction for a given deoxidant metal concentration [%R] corresponding to the average for steel,

B_m - average value of general coefficient of mixing in the reactive system,

D_R - coefficient of deoxidant diffusion.

In this approach the coefficient of deoxidant diffusion should account for the ratio of atomic weight of deoxidant and oxygen and the stoichiometry of reaction (10).

Equation (13) can be solved in the following way:

$$[\%O]_t = [\%O]_{eq} + ([\%O]_0 - [\%O]_{eq}) \cdot \exp(-B_m \cdot D_R \cdot t) \quad (14)$$

where: [%O]_t - present concentration of oxygen in liquid steel,

$[\%O]_0$ - initial concentration of oxygen in liquid steel.

In the computer calculation of the reactions, [%O]_t and [%O]₀ refer to the beginning and end of a given time step.

The segment of the model which is based on equations (10) - (14) describes the speed of the process for each metal separately by a distance of dissolved oxygen from the equilibrium concentration. The applied kinetic formula does not account for the nature of this process.

Then the products of deoxidation, i.e. non-metallic precipitates, flow out of steel. In each case bigger particles flow out faster, no matter the type of the flowing-out mechanism [13-15].

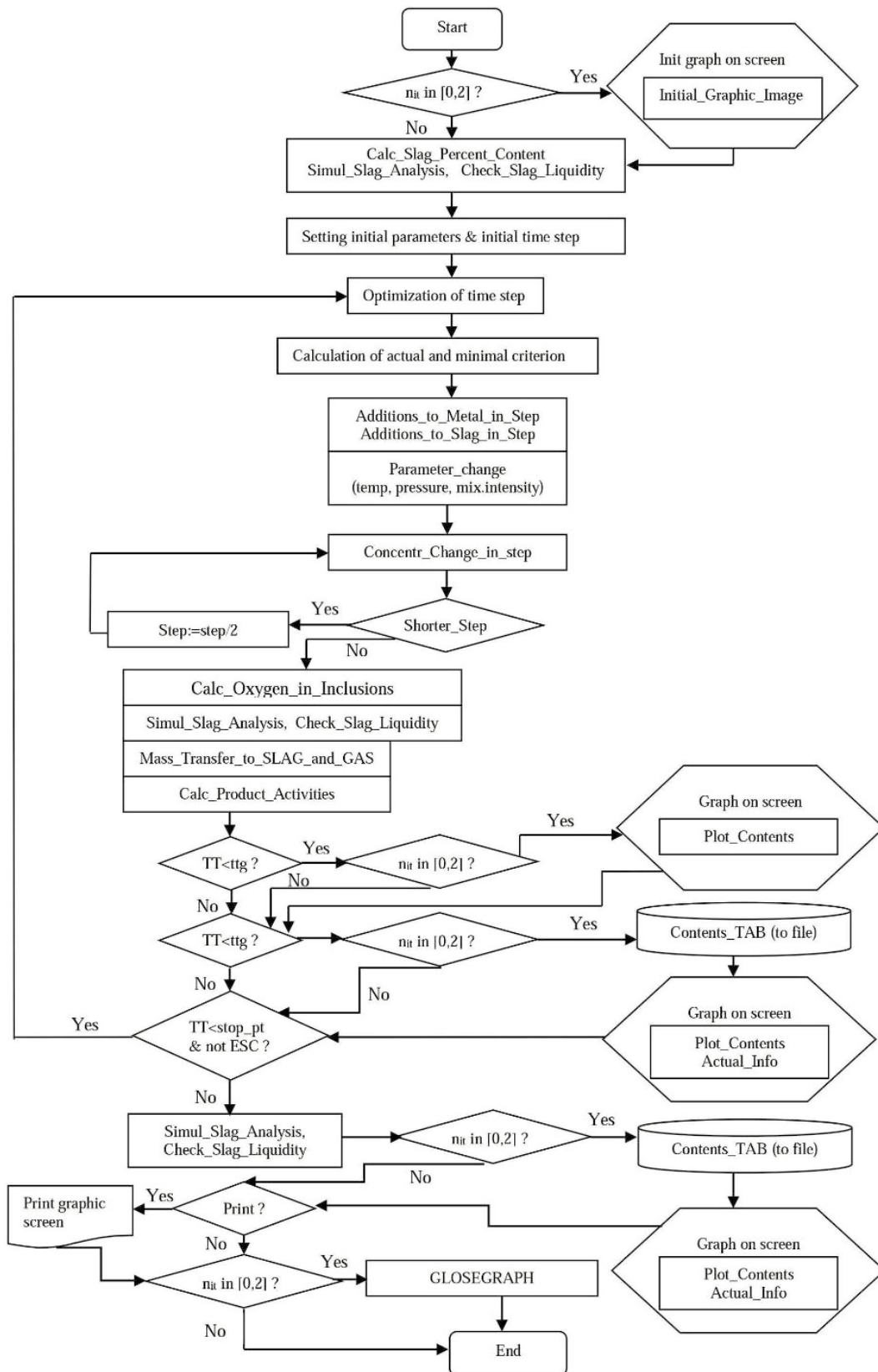


Figure 2. The block diagram of the simulation program WYK_Stal [13]

This program assumes a simple model of removal of oxidic precipitates. The model operates on wt% concentration of oxygen bonded by a given metallic component R - $[\%O]_R$. The difference between the present concentration and the expected value $[\%O]_{Rk}$ after a given stage of process of precipitate removal was assumed to be a driving force powering the process (13-14) [13, 17].

$$\frac{d[\%O]_R}{dt} = B_m \cdot C_R \cdot ([\%O]_R - [\%O]_{Rk})^n \quad (15)$$

In general, the value of average mixing coefficient B_m does not have to be identical as in equation (13), because the flowing out of inclusions also takes place after the flow-off is over, when the energy of mixing is lower. C_R denotes an individual outflow coefficient for $R_m O_n$. The introduction of this coefficient is justified by a differentiated character of inclusions, if the compounds appear in a pure form. Owing to the lack of experimental data, a common value was assumed for all types of inclusions, i.e. $C_R = 10^{-5} \text{ cm}^2/\text{s}$. The exponent n was assumed to be equal to 1.

The original version of the program was written in TurboPascal 7,0, with procedures in three basic modules: TL_SYM.PAS, TL_UZU.PAS, and TL_UZU_6.PAS. This computer software was composed of additional modules and such options as reactions of deoxidation, desulphurization, formation of nitrides, and verification results of calculation. The last option was used for checking out the behavior of the system in given conditions and for given reagents (21 components). The thermodynamic equilibrium was calculated with modules TLEN_PRO.EXE and TN_S_PRO.EXE [13-15, 17-18].

The calculations performed with WYK_STAL give results which are comparable with the industrial melting. The only parameter fitting the simulation to the real process in local conditions (size of the ladle, way in which metal bath is mixed) is an arbitrary component 'coefficient of mixing. This coefficient was fitted on the basis of ten or so melting processes of various types of steel, machined in a similar way. The starting point of simulations in liquid steel of defined mass, chemical composition and temperature. Alloy additives can be introduced only after their dosing is planned: continuous, by portions, or in one portion. In the analyzed system chemical reactions are observed, mainly oxidization of components and reactions with sulphur [4, 10-17].

3. Results of calculations

The current version of the program has been updated with thermodynamic data for rare earths metals and yttrium. The option to choose a calculation model has also been introduced. Preliminary results of calculations have been published in the conference

paper [18]. At the first stage calculations were made for the non-metallic phase formation for basic systems Fe-O-S-Al-Y and Fe-O-S-Al-Y-Ca. The program allows the choosing of a model for thermodynamic calculations [13, 17]:

- Model a: activity of the product of chemical reactions in liquid metal $a = 1$;
- Model b: coefficient of activity of components in liquid metal $f = 1$;

- Model c: account for partition coefficient L_S .

The calculations were conducted for models a and c in several variants:

Variation 1: First, 76 kg yttrium was added in the fifth minute, and 30 kg aluminum in the twentieth minute of the process. The first calculation series was performed with the use of model a. (figs. 3-5)

The results of calculations for O-S-Y-Al in model c are presented in figs. 6-8.

The change of order in which the additives were introduced resulted in great yttrium losses for the formation of the oxide phase. No sulfide phase formed because of the deficiency of yttrium needed for this process. No aluminum had to be added at the final stage of the process because the metal bath was strongly deoxidized by the first additive. Accordingly, this case was considered to be technologically unfavorable. Very similar calculation results were obtained for mode c and for model a. The presence of FeS was observed in non-metallic inclusions.

Table 2. Steel composition assumed for calculations [wt%][18]

Steel composition	C	Mn	Si	P	N	S
[wt%]	0.054	0.05	0.23	0.007	0.005	0.01

Table 3. Parameters of the deoxidation and desulphurization process[18]of yttrium reaction for temperatures 1575–1625°C [8]

process duration	30 minutes
weight of metal in ladle	140 000 kg
weight of slag	100 kg
temperature of metal at the beginning of the process	1670 °C
pressure of gaseous phase	1 atm
initial maximum oxygen bounded in inclusions	0.00%
initial total oxygen content in steel	0.01%
initial slag composition	CaO – 45%; Al ₂ O ₃ – 2%; MgO – 9%; MnO – 5%; SiO ₂ – 12%; FeO – 27%;
change of additives introduced to slag	100 kg SiO ₂ was added in the second minute



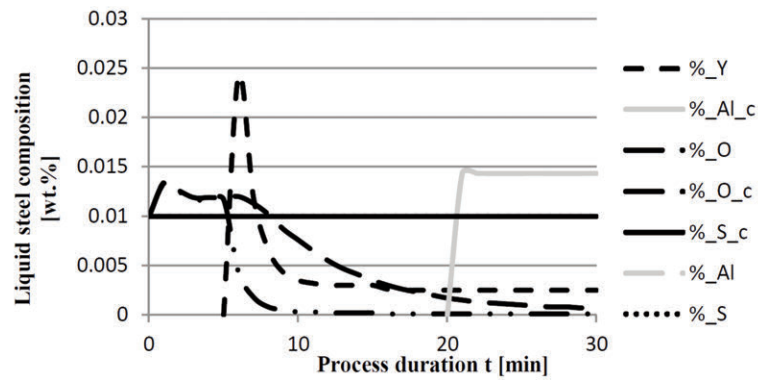


Figure 3. The variation of chemical elements concentration in liquid steel [wt.%] vs. process duration t [min]

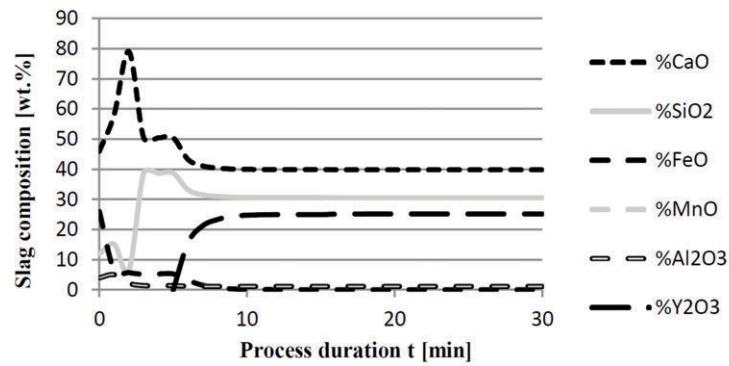


Figure 4. The variation of chemical composition of slag [wt.%] vs. process duration t [min]

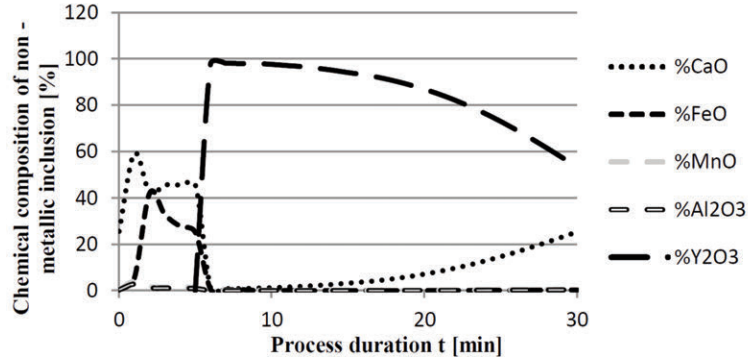


Figure 5. The variation of chemical composition of non-metallic inclusions [wt.%] vs. process duration t [min]

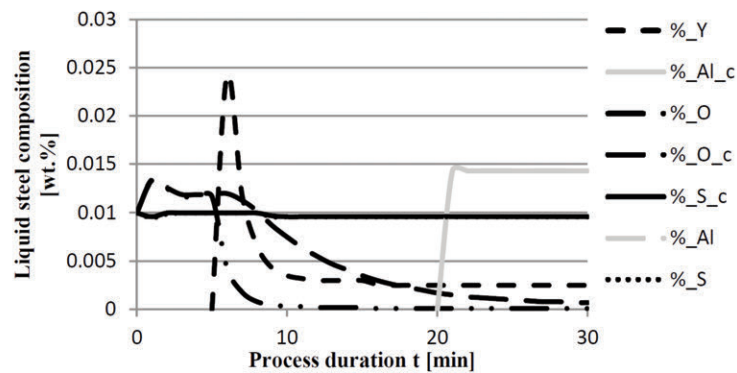


Figure 6. The variation of chemical elements concentration in liquid steel [wt.%] vs. process duration t [min]

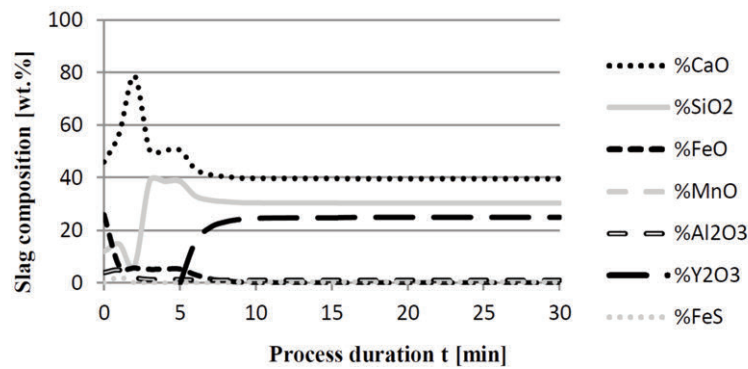


Figure 7. The variation of chemical composition of slag [wt.%] vs. process duration t [min]

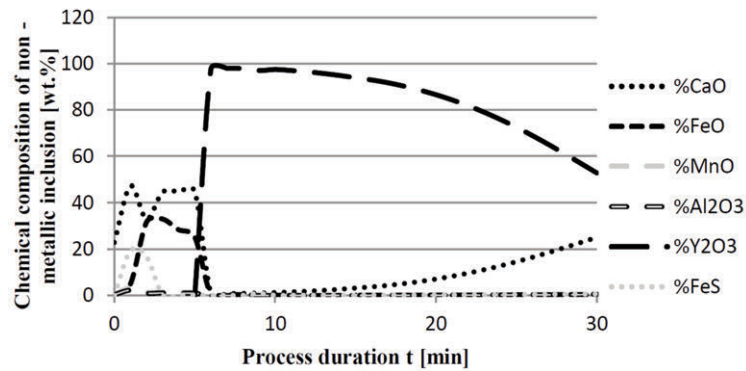


Figure 8. The variation of chemical composition of non-metallic inclusions [wt.%] vs. process duration t [min]

Then the refining process was analyzed for Fe-O-S-Al-Y-Ca system. The calculations were performed in the same way as in previous variants, except that calcium addition was taken into account. Calcium was introduced to modify the aluminum oxide inclusions and to desulphurize the metal bath, if necessary.

Variation 2: additives were introduced to steel in the following order: 30 kg aluminum in the first minute, 76 kg yttrium in the tenth minute, and 20 kg calcium in the twentieth minute. The results of the simulated refining process obtained for model a are presented in figs. 9-11.

Preliminary deoxidation with the use of aluminum lowered oxygen content to about 0.005%. Yttrium added in the tenth minute caused deep deoxidation; the drop of oxygen content was a result of yttrium consumption for sulfides formation. Calcium introduced at the end of the process also caused strong desulphurization of steel. These processes changed the chemical composition of non-metallic inclusions and slag. Oxides and sulfides were identified in slag. Sulfides were enriched with yttrium sulfide and calcium sulfide. Particularly interesting are the results of calculations obtained for non-metallic inclusions. The evolution of the composition was a consequence of introduced additives. A series of calculations performed for model c is presented in figs. 12-14. The obtained results of computer simulations are analogous to the results obtained for model a.

Variation 3: the same additive values were assumed, except that the order of dosing was changed: 30 kg aluminum was added in the first minute, after preliminary deoxidation 30 kg calcium was introduced in the tenth minute, and 76 kg yttrium in the twentieth minute of the process. The results of calculations for model a are presented in figs. 15-17.

The next calculation series was performed for model c.

The introduction of yttrium at the end of the refining process causes that less of this element is used for the formation of non-metallic phase; the addition of aluminum and then calcium suffice to reach a high level of deoxidation and desulphurization of liquid metal bath. Calculations performed for model a and c revealed that sulfide phase consists of CaS and FeS in model c, and CaS in model a, with the dominating role of the latter in inclusions. Its presence was also identified in slag.

3.1 Research of steel microstructure

The next stage of research included planning steel melting with the composition given in Table 4 with the addition of yttrium. The aim was to determine the effect of yttrium on the morphology and chemical composition of non-metallic inclusions, also in terms of limiting its losses to precipitation processes occurring in liquid steel and the formation of

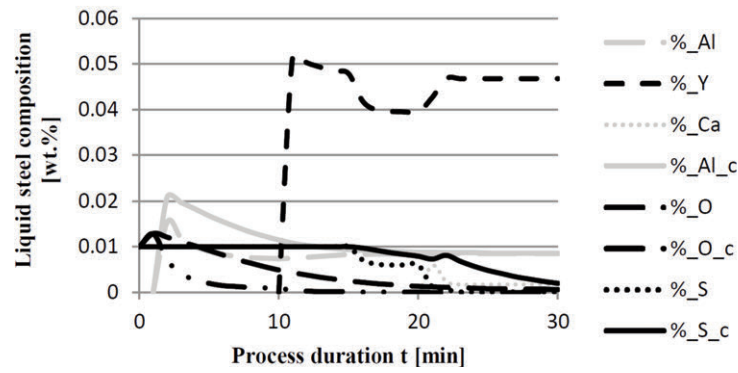


Figure 9. The variation of chemical elements concentration in liquid steel [wt.-%] vs. process duration t [min]

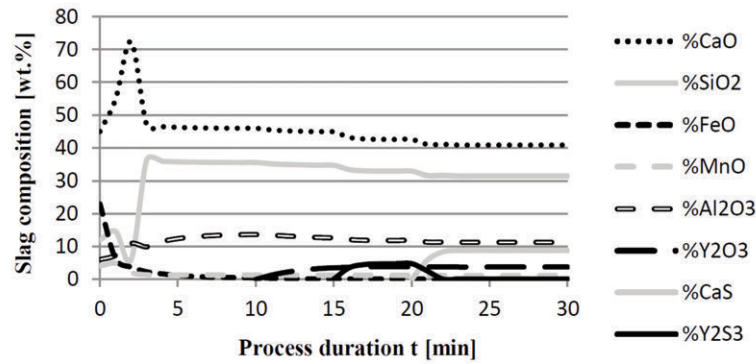


Figure 10. The variation of chemical composition of slag [wt.-%] vs. process duration t [min]

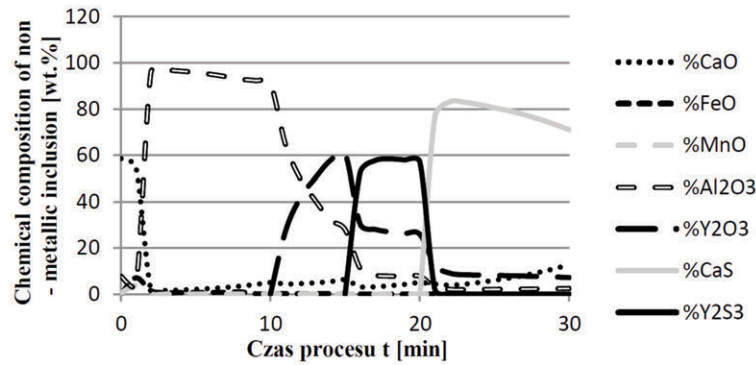


Figure 11. The variation of chemical composition of non-metallic inclusions [wt.-%] vs. process duration t [min]

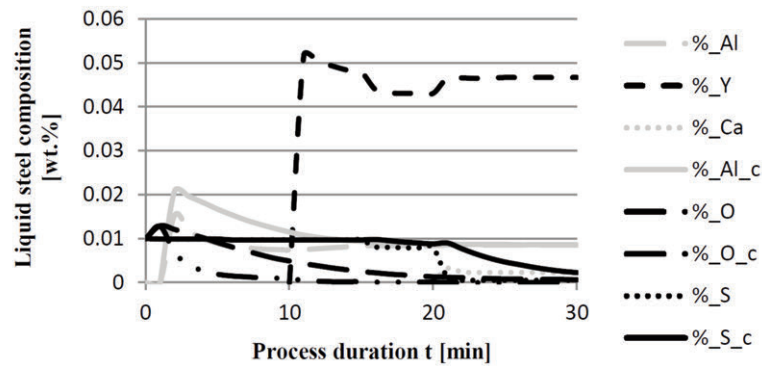


Figure 12. The variation of chemical elements concentration in liquid steel [wt.-%] vs. process duration t [min]

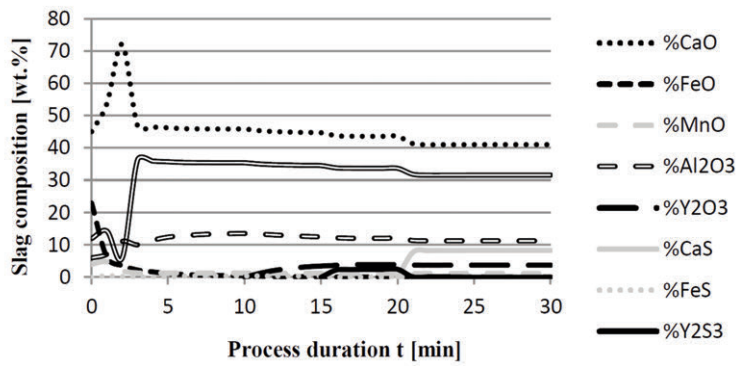


Figure 13. The variation of chemical composition of slag [wt.%] vs. process duration t [min]

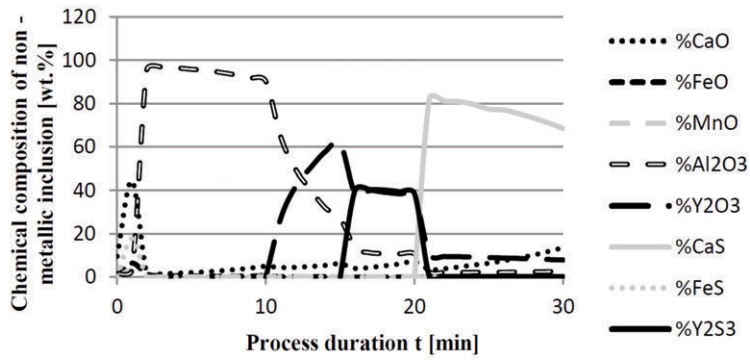


Figure 14. The variation of chemical composition of non-metallic inclusions [wt.%] vs. process duration t [min]

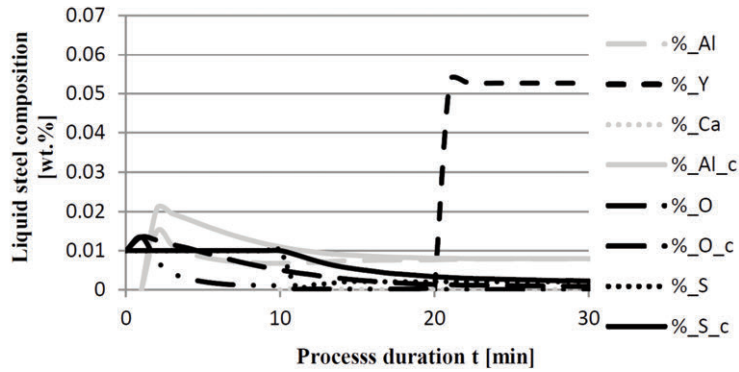


Figure 15. The variation of chemical elements concentration in liquid steel [wt.%] vs. process duration t [min]

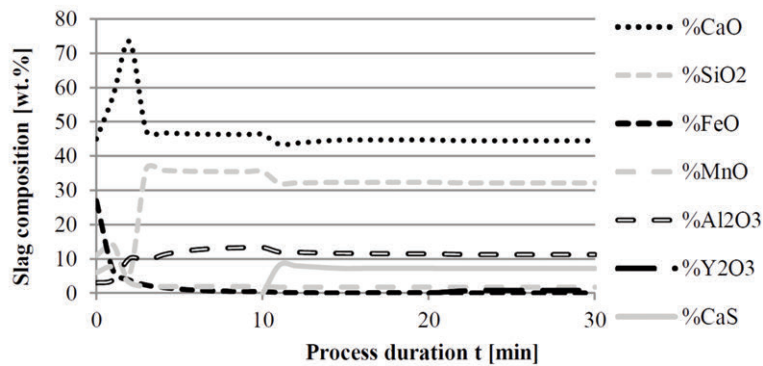


Figure 16. The variation of chemical composition of slag [wt.%] vs. process duration t [min]

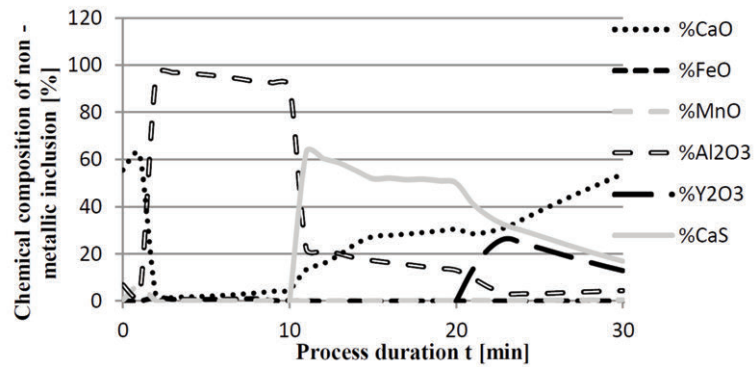


Figure 17. The variation of chemical composition of non-metallic inclusions [wt.%] vs. process duration t [min]

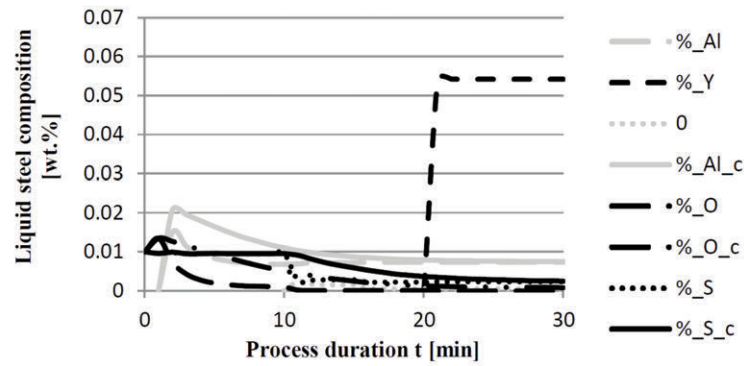


Figure 18. The variation of chemical elements concentration in liquid steel [wt.%] vs. process duration t [min]

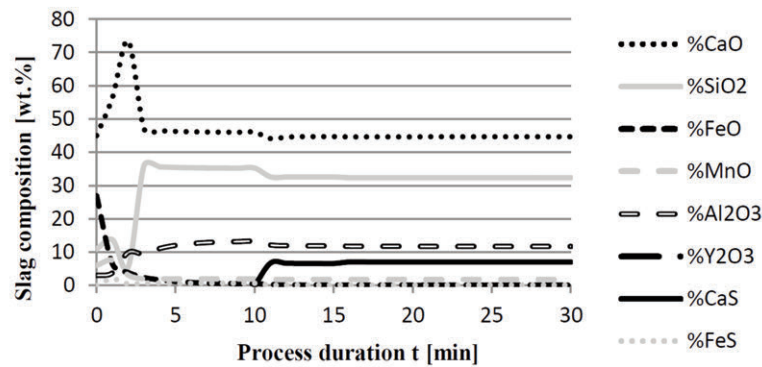


Figure 19. The variation of chemical composition of slag [wt.%] vs. process duration t [min]

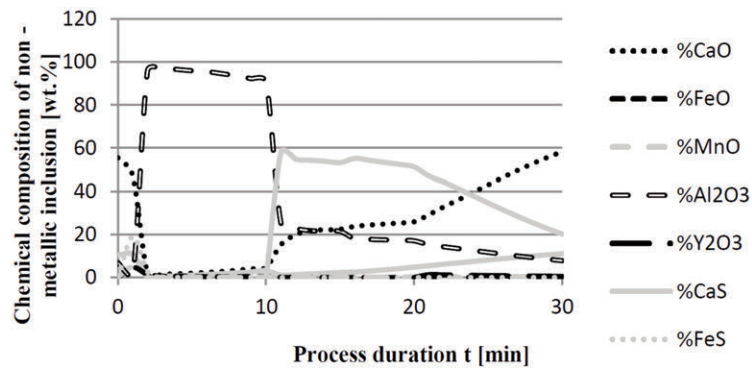


Figure 20. The variation of chemical composition of non-metallic inclusions [wt.%] vs. process duration t [min]

secondary inclusions. The laboratory melting was carried out in a vacuum furnace (vacuum furnace scheme shown in Figure 21).

After initial deoxidization, an addition of aluminum in the amount 0.7 g introduced 0.23 g of yttrium in metallic form, containing no admixtures of other elements. The total mass was $m = 700 + 0.7 + 0.23 = 700.93$ g. The time of melting and refining was 10 minutes. Then the melt was cast into a ceramic mold in argon atmosphere. Metal samples were taken from different areas of a cast ingot. Prepared samples after initial observation with an optical microscope were examined using a scanning electron microscope. The precipitants identified in a sample collected from the secondary metallurgy process were observed and chemically analyzed with the scanning electron microscopy with field emission FEI Quanta 3D, equipped with a detector EDS EDAX Apollo 40.

Nonmetallic inclusions typical of steel containing yttrium are presented in figures 22-33. The analysis of the obtained results shows that the precipitant in steel sample 1 (fig. 22) point 1 was composed of the yttrium compound. The situation is analogous for an inclusion in point 2 (fig. 23). High yttrium content in steel caused that the observed precipitants had a spherical shape. Inclusion labeled as 3 had a more complex character and was composed of complex manganese sulfide and yttrium sulfide. MnS precipitations were formed in the course of sulfur and manganese segregation processes, provided the equilibrium product of solubility was exceeded [4]. Hence the assumption that the observed inclusion was formed in the course of steel solidification after

adding yttrium, and after nucleation of MnS phase on yttrium sulfide. Yttrium sulfide is formed at the stage of refining, which precedes casting, including solidification, therefore presumably MnS can be separated on the existing sulfide inclusion, being a nucleation center of this phase. This does not exclude the simultaneous modification of inclusion with yttrium. The influence of rare soil elements on the crystalline structure of steel and modification of nonmetallic inclusions have been considerably well described in literature [17, 19]. The nonmetallic inclusions were mostly modified with rare soil elements, i.e. cerium and lanthanum, combination of rare soil elements (cerium, lanthanum, yttrium, neodymium, praseodymium, etc.), or mixture of selected metals, e.g. mischmetal. According to the experimental analyses, yttrium may also perform this function.

In the case of steel sample 2 (fig. 26) a cluster of fine inclusions was observed (points 3-6) and spherical inclusions, for which analyses were performed in points 1 and 2. Based on the obtained results the inclusions were identified as yttrium oxysulfides.

In sample 3 (fig. 30) the precipitant denoted as 1 contained Y, Al, O, and S. After adding Y to liquid steel, previously deoxidized with Al, Y might react with diluted Y and Al_2O_3 . This caused

Table 4 Chemical composition of steel [wt %]

C	Mn	Si	P	S	Al	O
0.71	0.89	0.23	0.023	0.028	0.0056	0.001

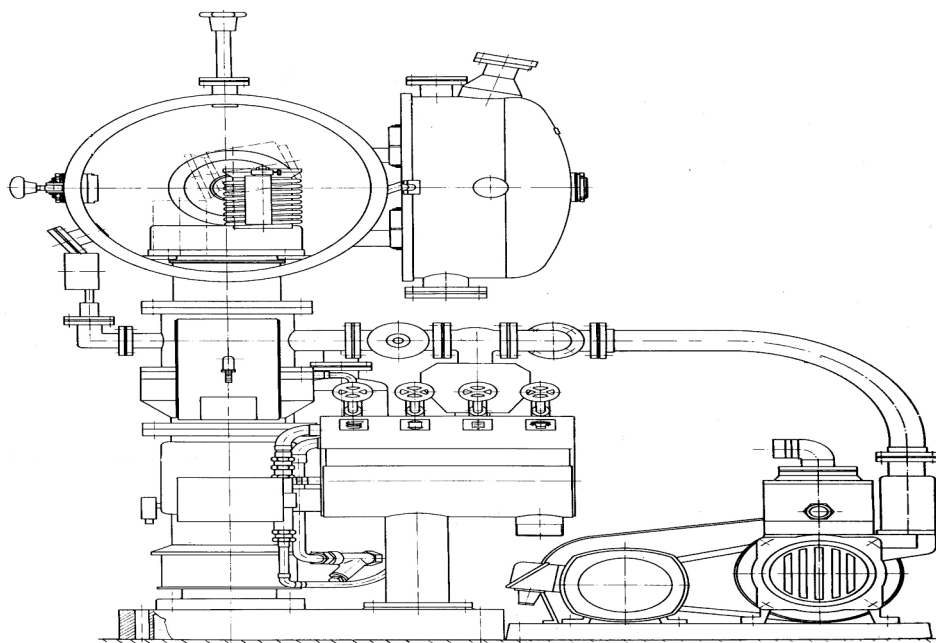


Figure 21. Scheme vacuum furnace



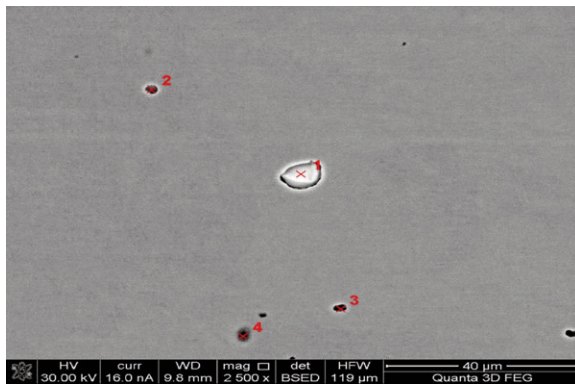


Figure 22. Microstructure of steel with the addition of yttrium obtained in scanning electron microscopy (SEM) concentration in liquid steel [wt.%] vs. process duration t [min]

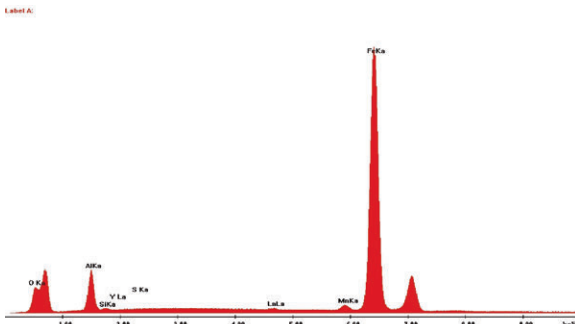


Figure 23. X-ray microanalysis spot chart obtained from the point 1 separation area

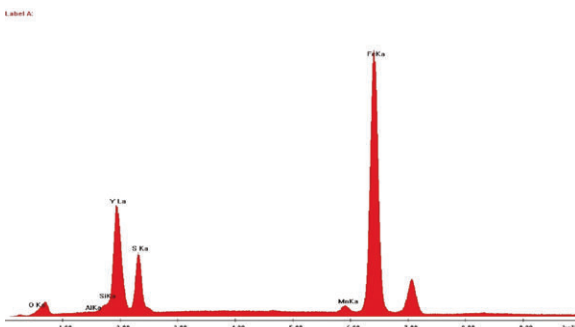


Figure 24. X-ray microanalysis spot chart obtained from the point 2 separation area

that complex inclusions $Y_2O_3 - Al$ and/or $Y_2O_3S - Al$ were formed, where the inner part was presumably enriched in Al, whereas the outer one in Y. This can be confirmed by a more detailed research analysis and thermodynamic analysis of nonmetallic precipitants after adding yttrium to liquid steel, which requires determining phases systems defining stability of produced compounds.

For obtaining reliable thermodynamic data on the stability of compounds with yttrium and reaction with

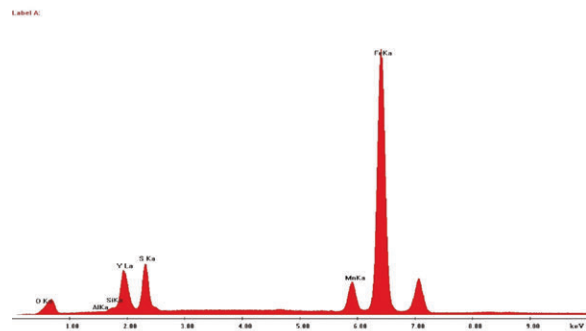


Figure 25. X-ray microanalysis spot chart obtained from the point 3 separation area

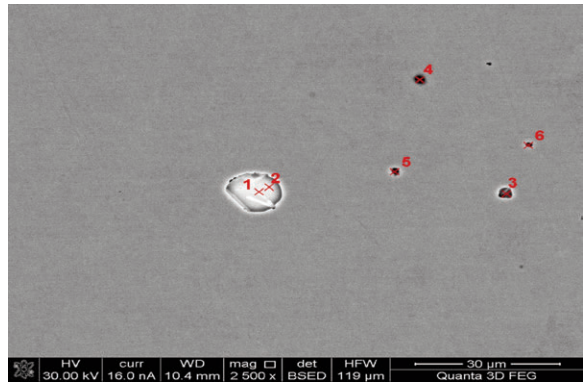


Figure 26. Microstructure of steel with the addition of yttrium obtained in scanning electron microscopy (SEM)

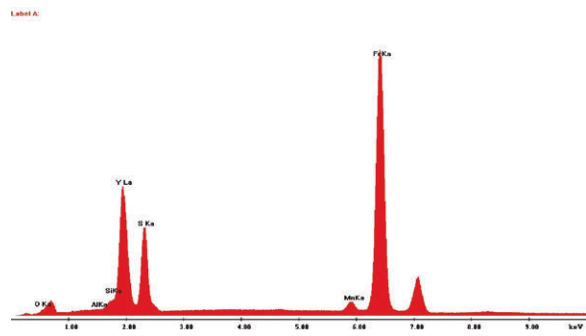


Figure 27. X-ray microanalysis spot chart obtained from the point 3 separation area

compound phases, e.g. oxides in its presence, the information about the build of oxitic compounds will be needed. First the basic double systems should be analyzed: $FeO-Y_2O_3$, and $Y_2O_3-Al_2O_3$, as well as the triple system $FeO-Y_2O_3-Al_2O_3$ [20]

The analysis of figure 34 reveals that after introducing yttrium and aluminum to steel at temperature 1600 °C, the deoxidizing products can be solid precipitants Y_2O_3 , $3Y_2O_3 \cdot 5Al_2O_3$, Al_2O_3 , and liquid oxitic phases [19-20].

The comparison of the results of experimental tests with simulations shows considerably similar

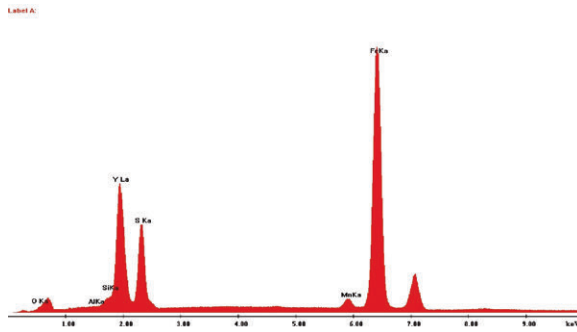


Figure 28. X-ray microanalysis spot chart obtained from the point 1 separation area

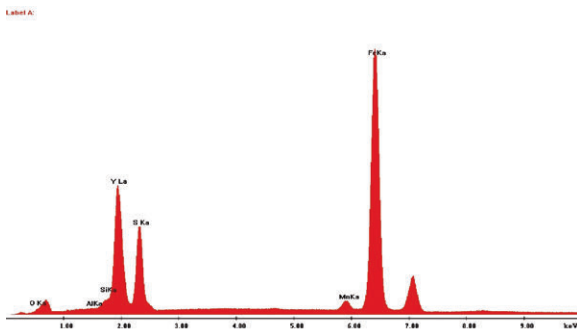


Figure 29. X-ray microanalysis spot chart obtained from the point 2 separation area

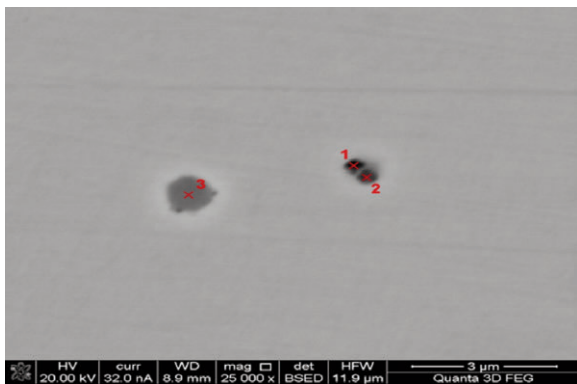


Figure 30. Microstructure of steel with the addition of yttrium obtained in scanning electron microscopy (SEM)

results of final elemental content in steel and nonmetallic phase in precipitants. Numerous spherical, minor non-metallic inclusions have been identified in the tested samples. Analysis of the chemical composition from the inclusion area showed that this phase contains elements: Y, O, and S, which suggests the formation of all three precipitates of oxide, sulphide, and yttrium oxysulfide. This means that the chemical composition of non-metallic inclusions is determined by the content of sulfur and oxygen, and the process of their formation probably includes phenomena associated with the segregation

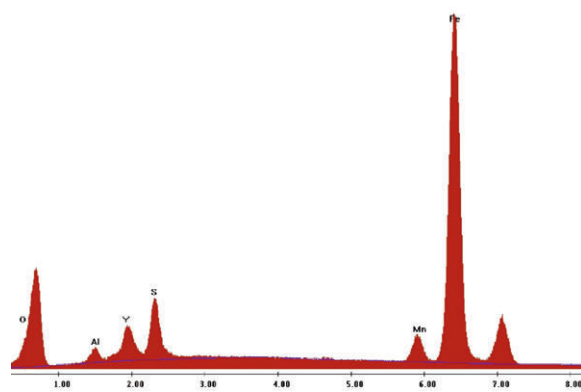


Figure 31. X-ray microanalysis spot chart obtained from the point 1 separation area

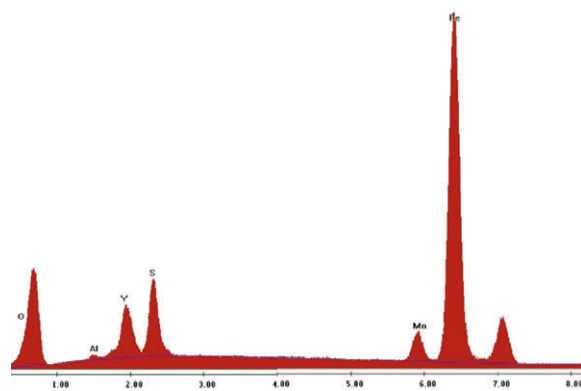


Figure 32. X-ray microanalysis spot chart obtained from the point 2 separation area

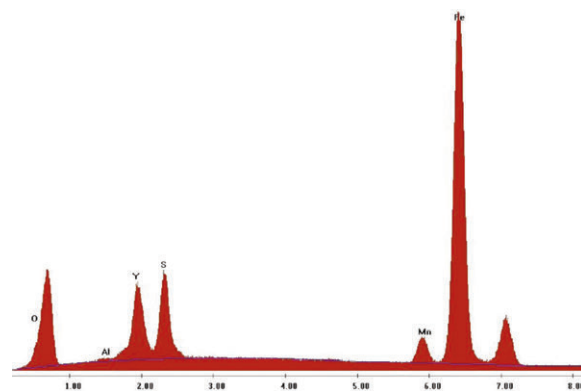


Figure 33. X-ray microanalysis spot chart obtained from the point 3 separation area

of these elements during solidification. It can therefore be assumed that the yttrium sulphide phase identified in the steel samples is a group of so-called secondary inclusions. In the case of yttrium oxysulfide discharges, it can be assumed that this compound is formed in an earlier stage before casting. The precipitation processes on the surfaces of existing non-metallic inclusions cannot be excluded. In the steel samples tested, there are no complex oxide

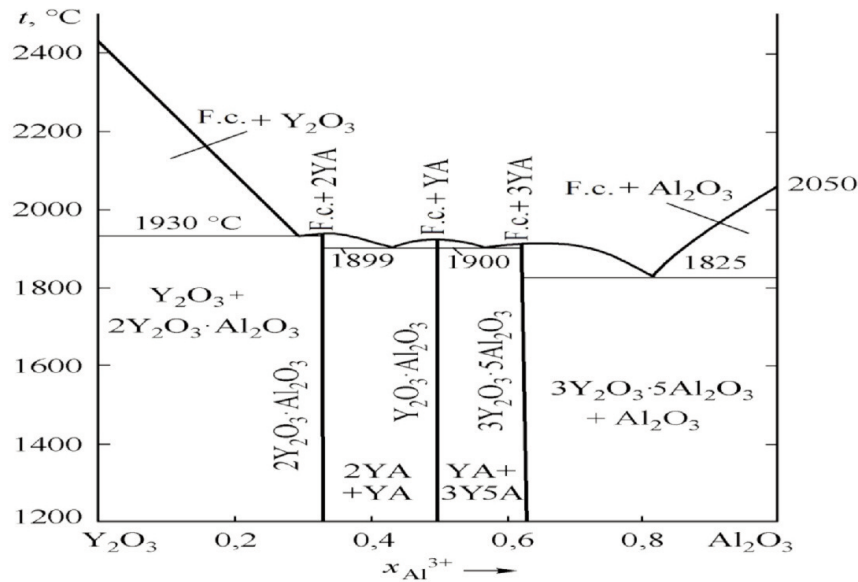


Figure 34. Phase system: Al_2O_3 - Y_2O_3 [20]

agglomerates, which confirms a properly conducted out-of-furnace treatment by applying a vacuum oven.

Fine precipitations of oxides, especially Y_2O_3 may play the role of a fine dispersive phase of solidifying character as well as crystallization and nucleation centers for other precipitations, e.g. nitrides and carbides. This signifies that their presence in this form could be advantageous for the efficiency of the process in certain conditions for definite types of steel. Sulfides may dissolve during thermal treatment of steel; deformation may also take place (e.g. MnS). This unfavorable phenomenon can be eliminated by adding yttrium and bonding it to Y_2O_2S . This compound does not dissolve, therefore prevents sulfur segregation on the grain interface and additionally causes precipitation hardening. MnS formation should be eliminated on behalf of hard Y_2S_3 and this should be done during refining and precipitation processes taking place in the course of solidification, which is not in the scope of this paper. This effect can be obtained by maintaining a definite level of oxygen and sulfur in liquid metal bath and formation of nonmetallic inclusions of strictly defined chemical composition and comminution. On the other hand the precipitation of yttrium compounds can be analyzed in view of yttrium losses caused by considerable chemical activity of this element. For this reason the adding of yttrium, control of the precipitation process and increase of inclusions can be treated as an important technological aspect which can be solved with mathematical models and informatics tools. Detailed simulation of steel refining will require further modification of the computer program by oxysulfides data.

4. Conclusions

Upon a simultaneous addition of yttrium and aluminum to liquid steel, the Al_2O_3 content was observed to remain on the same level. This means that yttrium losses were considerable when oxide phases were formed. This effect was reinforced by elevated sulphur content in the system, resulting in yttrium sulfide formation.

The yttrium sulfide formation at a low oxygen content eliminated the process of manganese sulfide formation. For the sake of limiting yttrium losses for the sulfides formation, the metal bath had to be completely desulphurized.

The obtained sulfide inclusions on the basis of yttrium had different shape compared to the elongated MnS inclusions.

The yttrium and sulfur compounds were in the form of small spherical phases evenly distributed in a cast ingot.

The addition of yttrium and the formation of simple and complex compounds with sulfur eliminated the process of MnS formation in steel.

References

- [1] A. Costa e Silva, J. Min. Metall. Sect. B-Metall., 52 (1) B (2016) 41-46.
- [2] R. Pereira Batista, A. Augusto – Martins, A. L. V. Costa e Silva, J. Min. Metall. Sect. B-Metall. 53(3) B, (2017), 357-363.
- [3] Q. Wanga, L.J. Wanga, YQ. Liuc, K.C. Chou, J. Min. Metall. Sect. B-Metall., 53(3) B (2017) 365-372.
- [4] D. Kalisz: Termodynamiczna charakterystyka powstawania fazy niemetalicznej w ciekłej stali Wyd. Naukowe Akapit, Krakow, 2013, p. 193.
- [5] A. D. Pelton, S. A. Degterov, G. Eriksson, C. Robelin,



- Y. Dessureault, Metall. and Mat. Trans. B, 31 B (2000) 651-659.
- [6] A. D. Pelton, Y. B. Kang, Int. J. Mat. Res. 98 (10) (2007) 1-11.
- [7] A. Costa e Silva, J. Min. Metall. Sect. B-Metall., 35 (1B) (1999) 85-112.
- [8] W. Longmei, D. Ting, Y. Kexiang, Inorg. Chim. Acta, 140 (1-2) (1987) 189-191.
- [9] G. G. Mikhailov, L. A. Makrovets, L.A. Smirnov, Bulletin of the South Ural State University. Ser. Metallurgy, 16 2 (2016) 5-13.
- [10] T. Du, L. Wang, J. Less Common Met., 110 (1985) 179-185.
- [11] J. Iwanciw, Acta Metallurgica Slovaca, 5 (2007) 172-176.
- [12] J. Iwanciw, Simulator of steelmaking processes for work in real time, Komitet Metalurgii PAN, Wyd. Nauk. Akapit, Krakow (1) 2002 p. 186-192.
- [13] Program instructions WYK_STAL.
- [14] J. Iwanciw, D. Podorska, J. Wypartowicz, Arch. Metall. Mater., 56 (4) (2011) 999-1005.
- [15] J. Iwanciw, D. Podorska, J. Wypartowicz, Arch. Metall. and Mater., 56 (3) (2011) 635-644.
- [16] D. Podorska, P. Drożdż, J. Falkus, J. Wypartowicz, Arch. Metall. Mater. 51 (4) (2006) 581-586.
- [17] S. Gerasin, Evolution of chemical composition and model of growth non-metallic inclusions in liquid steel with yttrium content. Dissertation. AGH-UST, Krakow, 2017, p.163.
- [18] S. Gerasin, D. Kalisz, P. L. Żak, J. Iwanciw, 5th IOP Conf. Ser.-Mat. Sci., 461 (1) (2019) p.1-6.
- [19] L. A. Smirnov, V. A. Rovnushkin, A. S. Oryshchenko, G. Y. Kalinin, Metallurg, 11 (2015) 57-63.
- [20] G. G. Mikhailov, L. A. Makrovets, L. A. Smirnov, Bulletin of the South Ural State University, Ser. Metallurgy, 14 (4) (2014) 5-10.

TERMODINAMIČKA I KINETIČKA SIMULACIJA FORMIRANJA NEMETALIČNE FAZE Y_2O_3 I Y_2S_3 U TEČNOM ČELIKU

S. Gerasin, D. Kalisz*, J. Iwanciw

* AGH Univerzitet prirodnih nauka i tehnologije u Krakovu, Poljska

Apstrakt

U ovom radu je ispitivano formiranje nemetaličnih uključaka koji su nastali kao rezultat dodavanja itrijuma kao legirajuće komponente u tečni čelik. Redosled dodavanja određenih komponenti određuje njihov konačni sadržaj u čeliku, i ovaj problem je analiziran pomoću WYK_Stal programa koji je razvijen na AGH Univerzitetu prirodnih nauka i tehnologije u Krakovu. Ispitivana je Y_2O_3 i Y_2S_3 faza precipitacije, kao i odnos između dodavanja Y, Al, Ca, O, i S u rastopljeni čelik pomoću termodinamičkih modela koji se zasnivaju na Vagnerovoj teoremi. Uvođenje itrijuma pre dodavanja aluminijuma dovodi do velikih gubitaka usled formiranja oksida. Niski sadržaj kiseonika u metalnoj kupki pospešuje formiranje itrijum sulfida. Kada se itrijum uvede nakon aluminijuma i kalcijuma, on doprinosi taloženju svog sulfida, i na ovaj način se smanjuje formiranje manganovog sulfida.

Ključne reči: Itrijum; Nemetalični talog; Čelik; Kompjuterska simulacija

